Applied Surface Science 525 (2020) 146610

Contents lists available at ScienceDirect

Applied Surface Science

journal homepage: www.elsevier.com/locate/apsusc

Chemical bonding at room temperature via surface activation to fabricate low-resistance GaAs/Si heterointerfaces

Yutaka Ohno[a,*], Jianbo Liang[b], Naoteru Shigekawa[b], Hideto Yoshida[c], Seiji Takeda[c], Reina Miyagawa[d], Yasuo Shimizu[e], Yasuyoshi Nagai[e]

[a] Institute for Materials Research (IMR), Tohoku University, 2-1-1 Katahira, Aoba-ku, Sendai 980-8577, Japan
[b] Graduate School of Engineering, Osaka-City University, 3-3-138 Sugimoto, Sumiyoshi, Osaka 558-8585, Japan
[c] The Institute of Scientific and Industrial Research (ISIR), Osaka University, 8-1 Mihogaoka, Ibaraki, Osaka 567-0047, Japan
[d] Department of Physical Science and Engineering, Nagoya Institute of Technology, Gokiso-cho, Nagoya 466-8555, Japan
[e] Institute for Materials Research (IMR), Tohoku University, 2145-2 Narita-cho, Oarai, Ibaraki 311-1313, Japan

ARTICLE INFO

Keywords:
Low-temperature direct wafer bonding
Surface activation
Heterointerfaces
Scanning transmission electron microscopy
Low-temperature focused ion beam

ABSTRACT

Bonding mechanism at room temperature (RT) in GaAs/Si heterointerfaces fabricated by surface-activated bonding (SAB) is examined using cross-sectional scanning transmission electron microscopy combined with low-temperature focused ion beam and time-of-flight secondary ion mass spectrometry. In the bonding process at RT, atomic intermixing at the interfaces, presumably due to the transient enhanced diffusion assisted by the point defects introduced in the surface activation process, is confirmed. The defect-assisted atomic diffusion at the interfaces, as well as the formation of atomically clean and activated surfaces, would be the key concept of SAB, by which we can create tough heterointerfaces at RT. Meanwhile, the defects on the activated surfaces would degrade the interface resistance. The degraded properties can be recovered by an appropriate annealing after the SAB processes, although the atomistic structure around the heterointerfaces would be modified during the annealing. By controlling SAB and subsequent annealing conditions, we can obtain low-resistance heterointerfaces via the optimization of the trade-off relationship between the chemical bonding strength and the electronic properties, determined by the activated surfaces before bonding.

1. Introduction

Surface-activated bonding (SAB), that is a direct wafer bonding process without additional buffer layers [1], is a promising method to fabricate tough and steep heterointerfaces at low cost. SAB does not require annealing processes to obtain sufficient bonding strength, unlike in the most other direct bonding processes such as hydrophilic, hydrophobic and plasma-assisted bonding, except for gold-gold hydrophilic bonding [2]. This low-temperature process does not induce thermal damage at the interfaces. In addition, unlike in epitaxial growth processes, SAB can fabricate any heterointerfaces free from threading dislocations, even for dissimilar materials with different crystal structures and lattice constants. Recently, SAB is applied to the next-generation semiconductors such as diamond [3], SiC [3–7], and GaN [8–10], as well as to the basic semiconductors such as Si and GaAs [11–14], towards low-resistance semiconductor-to-semiconductor heterointerfaces free from adherent layers. Functional devices with hybrid structures, such as high-power semiconductor lasers with a low interface thermal resistance [4] and high-efficiency tandem solar cells with a low interface electrical resistance [15,16], are so far demonstrated with this direct bonding method.

Since SAB processes are based on the chemical bonds between two wafer surfaces obtained using surface activation, the surfaces are required to be atomically clean and activated, as well as flat and smooth sufficiently. Therefore, in general SAB processes, wafer surfaces are activated at low temperatures before bonding by creating dangling bonds via the irradiation of inert atoms in a high vacuum, and the surfaces are then bonded by the contact most of the time under pressure to form strong chemical bonds even for imperfect surfaces. During the activation process, however, atomic arrangement beneath the irradiated surfaces can be modified, depending on the irradiation conditions such as inert atom species with different kinetic energies. This structural modification would result in the degradation in physical properties of the interfaces, especially in the electronic properties such as interface resistances. Therefore, SAB processes have been optimized empirically the trade-off relationship between the chemical bonding

* Corresponding author.
E-mail address: yutakaohno@imr.tohoku.ac.jp (Y. Ohno).

https://doi.org/10.1016/j.apsusc.2020.146610
Received 19 March 2020; Received in revised form 5 May 2020; Accepted 5 May 2020
Available online 06 May 2020

strength and physical properties depending on bonded materials. Even though SAB has been applied for any kinds of materials, the principle of the trade-off relationship has been controversial due to the difficulty of analyzing their nonequilibrium heterostructures at an atomistic level.

In the present work, we have examined the atomistic structure of SAB-fabricated GaAs/Si heterointerfaces towards tandem solar cells, that can surpass the efficiency milestone of 30% for non-concentrating terrestrial solar cells free from expensive Ge wafers [17–19]. Nowadays, InGaP/GaAs//Si hybrid multijunction cells with a high efficiency up to 26% are demonstrated with the SAB method [15,16]. However, the estimated efficiency is still lower than the theoretical one of 40% [20]. One possible origin of this lower efficiency is the interface resistance of the order of 10^{-1} Ωcm^2 [14,21], which is rather high in comparison with III-V/IV heterointerfaces grown epitaxially (of the order of 10^{-4} Ωcm^2) [22]. The resistance is decreased by annealing at low temperatures [13,14,23,24], indicating the annihilation of defects at the interfaces. It is pointed out that defective regions at the interfaces would affect the electrical properties [23]. Actually, volume of the regions, depending on inert atom species and activation times [12,25,26], correlates with the interface resistance [12]. Recently, plane-view transmission electron microscopy (TEM) with damage-free TEM specimens fabricated by chemical mechanical polishing (CMP) techniques shows that, As defects on the activated GaAs surfaces would be an origin of the interface resistance in a SAB-fabricated GaAs/Si heterointerface [27]. We have therefore examined the atomic arrangement and composition around similar GaAs/Si heterointerfaces deliberately by cross-sectional scanning TEM (X-STEM) combined with low-temperature focused ion beam (LT-FIB) technique that can suppress the structural modification during FIB processes [28]. With an assistance of time-of-flight secondary ion mass spectrometry (TOF-SIMS), atomic structures involving point defects at the interfaces, determined by the SAB condition, are discussed.

2. Experimental methods

GaAs/Si heterointerfaces, and GaAs/GaAs and Si/Si homointerfaces were fabricated at room temperature (RT) in a high vacuum (below 5 × 10^{-5} Pa), with the rectangular wafers (about 10 mm × 15 mm in size) of Si-doped n-type (1 0 0) GaAs (with a carrier concentration of 2 × 10^{16} cm^{-3}) and B-doped (1 0 0) p-Si (2 × 10^{14} cm^{-3}), under the similar SAB conditions. The wafers were activated with a beam of inert Ar atoms (with a current of 1.8 mA at an applied voltage of about 2.0 kV) for 180 s (with the dose of 2 × 10^{18} atoms/cm^2 at the atom energy of 2 keV), with the incident angle of 45°, and they were then pressed for 60 s at 10 MPa for bonding. The activated surfaces might be contaminated with a small amount of metallic impurities from the susceptors, although they were hardly detected around the interfaces fabricated with an optimum SAB condition by atom probe tomography of which the detection limit is about 0.01 at.%. In order to examine a possible distribution of impurity atoms after the SAB processes, some amount of Fe atoms was intentionally introduced in the surface activation process, by the irradiation of Ar atoms on the susceptors simultaneously with the wafers. The Fe concentration at the surface was estimated to be the order of a few % by atom probe tomography techniques [29]. A part of the interfaces was annealed at 400 °C for 60 s in a nitrogen gas ambient, since the electric resistance of our interfaces is minimized with this optimum annealing condition [14].

Specimens for X-STEM with GaAs/GaAs [30] and Si/Si [31] homointerfaces were prepared only by CMP techniques, by which no irradiation damage would be introduced [30]. Meanwhile, X-STEM specimens with GaAs/Si heterointerfaces were hardly prepared by CMP, since the etching rate for Si was more than 10 times higher than for GaAs. They were therefore prepared by using a focused ion beam (FIB) system equipped with a high-resolution scanning electron microscope (SEM) (FEI, Helios NanoLab600i) with Ga^+ ions accelerated at 2–30 kV [32], with a cold stage operated at a low temperature (LT) of −150 °C (IZUMI-TECH, IZU-TSCS004) to suppress the defect generation in the FIB processes [28]. SEM revealed the FIB specimens of uniform thickness across the interface. Structural properties of the interface were determined by high-angle annular dark-field (HAADF) and energy dispersive x-ray spectroscopy (EDX) under STEM with the incident direction of ⟨1 1 0⟩, with a JEOL JEM-ARM200F analytical microscope. By using STEM-EDX, we detected the x-rays due to Fe atoms localized at bonded interfaces. Even though the peak density of Fe atoms varies area by area, the full-width at half-maximum (FWHM) of the Fe distribution was almost the constant value of 1 nm. Even though the spatial resolution of STEM-EDX would depend on the specimen thickness via the spread of electron beam, the FWHM was independent of the specimen thickness. This suggests that the spatial resolution of our STEM-EDX was less than 1 nm.

To discuss the defect generation at GaAs surfaces in the activation process, the depth profile of the As/Ga density ratio, as well as the Fe density, was examined from the activated surfaces by TOF-SIMS, using a PHI TRIFT V nanoTOF (ULVAC-PHI). An area of 1 × 1 mm^2 was sputtered with a beam of O_2^+ ions accelerated at 1 kV (with a current of 100nA) to obtain positive ion depth profile, and areas of 0.1 × 0.1 mm^2 in the sputtered area were measured with Bi_3^{++} ions accelerated at 30 kV.

3. Results and discussions

3.1. As-bonded GaAs/Si heterointerfaces

Distribution of As defects and Fe atoms beneath an activated GaAs surface, just before bonding, is examined by TOF-SIMS (Fig. 1). The As/Ga ratio is 0.8 on the surface. It increases with increasing the depth from the surface, and reaches to 1.0 at the depth of 3 nm. This result indicates the introduction of As vacancies beneath the surface, as reported in SAB-fabricated GaAs/GaAs interfaces [27]. Meanwhile, the ratio is above 1.0 in the depth range of 3–7 nm, suggesting that As interstitials would be introduced in the deeper region. Those results can be explained that Frenkel-type defects (i.e., vacancy-interstitial pairs) on the As sites are introduced due to knock-on effects under the irradiation of Ar atoms for surface activation. Besides, Fe atoms would locate just on the activated surface and they do not penetrate the surface so much.

Even though Ar atoms would remain in the activated surfaces [12], they are scarcely observed in our experiments. The distribution of Ar atoms in the surfaces can be simulated with the SRIM software [33], and the density of the residual Ar atoms would peak at the depth of 3 nm. The simulation also suggests the introduction of vacancies of which density is the maximum at the depth of 1.5 nm. Those results are consistent with the TOF-SIMS result shown in Fig. 1.

Meanwhile, distribution of point defects beneath an activated Si surface is hardly examined by TOF-SIMS, because the surface is easily oxidized after the surface activation process. It is known that the surface would be amorphized during the activation process [13,25–27]. Since Fe atoms are immobile in amorphous Si at RT [34], Fe impurities

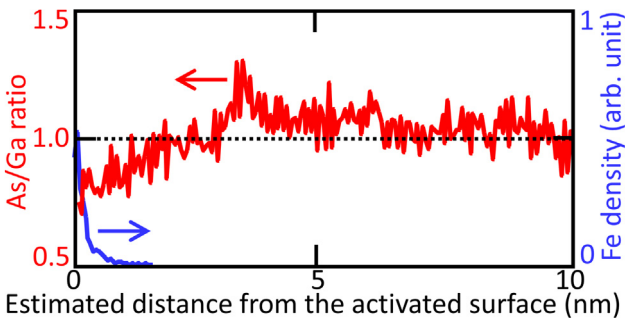

Fig. 1. Depth profile of the As/Ga ratio and Fe density in GaAs after the surface activation process, obtained by TOF-SIMS.

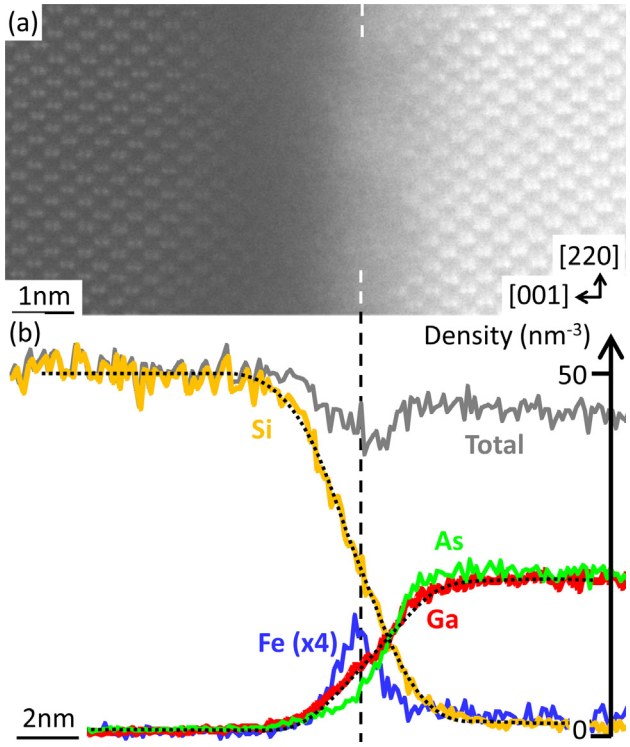

Fig. 2. (a) HAADF-STEM of an as-bonded GaAs/Si interface. (b) Density profiles across the interface for As (the green curve), Ga (red), Si (orange), Fe (blue), and all kinds of atoms (grey), obtained by energy dispersive x-ray spectroscopy (EDX). (For interpretation of the references to colour in this figure legend, the reader is referred to the web version of this article.)

would locate just on the surface, as on the activated GaAs surfaces. Also, SRIM calculations suggest that vacancies are introduced by the Ar atom irradiation by which the density of residual Ar atoms would peak at the depth of 4 nm, and the density of Si vacancies would be the maximum at the depth of 2 nm.

Fig. 2(a) shows a HAADF-STEM image of an as-bonded GaAs/Si heterointerface. EDS in the LT-FIB specimen reproduces a steep heterointerface (Fig. 2(b)), unlike in the specimens fabricated by the conventional FIB operated at RT (see Fig. S1 in the supplementary materials (SM)). The density gradients for Si, Ga, and As atoms at the interface in the LT-FIB specimen (about 20% nm^{-1}) are much larger than those in the RT-FIB specimen fabricated in our experiments (about 9% nm^{-1}). Those gradients indicate a slight atomic intermixing across the interface in the bonding process. It is therefore difficult to determine the exact location of the interface with the density profiles. We hypothesize that the Fe density is the maximum just on the interface (the broken line in Fig. 2(b)), because Fe atoms would locate on the activated surfaces before bonding. Under the hypothesis, the density profiles for Ga and Si atoms can be fitted well with an error function of the distance x from the expected interface, $C_0\mathrm{erfc}[x/(2L)]$ (the dotted curves in Fig. 2(b)), which is the solution of the one-dimensional diffusion equation for a diffusion constant L and for a semi-infinite source with a constant density of $2C_0$ at $x > 0$ [35]. The density profile for As atoms is not explained with the simple diffusion model, and it is discussed later.

In the GaAs wafer adjacent to a GaAs/Si interface, no amorphous layer is introduced, and lattice fringes are observed even in the vicinity of the interface (Fig. 2(a)). Vacancy agglomerates about 1 nm in size can be observed as dark dots nearby the interface. The ratio between the As density and the Ga one, As/Ga, is below 1.0 down to the depth of 2 nm from the interface, and it is above 1.0 in the depth range of 2–6 nm (Fig. 2(b)), due to Frenkel-type defects on the As sites (Fig. 1). Similar properties are obtained in SAB-fabricated GaAs/GaAs interfaces in damage-free STEM specimens (see Figs. S2(a) and (b) in the SM). Therefore, the GaAs wafer adjacent to an interface would not be damaged severely in the LT-FIB process [28]. Meanwhile, atomic migration would take place due to recombination effects in the process [28]. While the diffusion length of Fe atoms L_{Fe} in the bonding process can be estimated to be 0.7 nm, as the FWHM of the density profile for excess Fe atoms in GaAs [35], this value is slightly larger in comparison with the damage-free GaAs/GaAs interfaces in a specimen fabricated without FIB (see Fig. S2(b) in the SM). The upper limit of the diffusion length of Si atoms L_{Si} in the bonding process is estimated to be 0.8 nm by fitting the density profile for Si atoms with an error function, and the estimated value is close to the full-width at half maximum (FWHM) of the density profile for excess Si atoms in GaAs. Assuming that the T-dependence of the diffusion constant reported at high temperatures for Si [36] and that for Fe [37] are conserved even at low temperatures, both L_{Si} and L_{Fe} in the bonding process are expected to be the order of 10^{-10} nm at RT. This suggests a transient enhanced diffusion due to the point defects introduced in the surface activation process, as observed in implanted GaAs wafers [38]. The distribution range of As vacancies beneath the activated surfaces is decreased by about 1 nm in the bonding process, indeed (see Figs. 1, 2(b) and S2 in the SM).

In the Si wafer adjacent to a GaAs/Si interface, an amorphous layer of a few nm thick is formed (Fig. 2(a)), similar to SAB-fabricated Si/Si interfaces (see Fig. S3(a) in the SM) [13,25–27]. The L_{Fe} in the boning process, estimated to be 0.8 nm as the FWHM of the density profile for excess Fe atoms in Si [35], is the same as the L_{Fe} in damage-free Si/Si interfaces (see Fig. S3(b) in the SM), since recombination effects would be ignored in Si [28]. The diffusion length of Ga atoms L_{Ga} in the bonding process can be estimated to be 0.8 nm by fitting the density profile for Ga atoms with an error function, as well as with the FWHM of the density profile for excess Ga atoms in Si (Fig. 2(b)). Meanwhile, the density profile for As atoms is not fitted with an error function, since the As density beneath the activated GaAs surface before bonding is not constant (Fig. 1). We hypothesize that the FWHM of the density profile for excess As atoms in Si approximates the diffusion length of As atoms L_{As} in the bonding process. Under the hypothesis, L_{As} is estimated to be 0.8 nm. Interestingly, Fe, Ga, and As atoms in Si have the same diffusion length of 0.8 nm in the bonding process. Considering the diffusion constants at high temperatures in Si for Ga [39] and As [40], as well as the diffusivity in Si for Fe atoms [30], those atoms should be immobile at RT. Those results can be explained with a transient enhancement model that the diffusion lengths of those impurities are dominated by the diffusivity of the point defects assisting the impurity diffusion, like a transient enhanced diffusion in Si [41].

Fig. 2(b) also shows the total sum of densities for all kinds of atoms across the interface. The density far from the interface is $8/(0.565)^3$ nm^{-3} in the GaAs side, while it is $8/(0.543)^3$ nm^{-3} in the Si side. The density varies gradually at the interface, and an intermediate layer of 4–5 nm thick having gradient composition is formed. One possible explanation is that this layer would be formed such that lattice mismatch between GaAs and Si does not result in a highly defective interface with a high energy; i.e., it would act as a buffer layer that can reduce the elastic energy around the interface. However, by using a direct bonding method using atomically-flat surfaces formed thermally without the surface activation process, GaAs/Si heterointerfaces free from an apparent gradient layer can be formed at RT [42]. This suggests that the main origin of the formation of a gradient layer is not to minimize the interface energy. Another possible explanation is that a gradient layer can be formed due to the influence of the roughness on the activated surfaces. In order to maximize the chemical bonds at the interface, atoms would diffuse so as to fill the rough bonding interface during the bonding process. In this case, atomic diffusion would take place within a surface region of which thickness is the order of the peak to valley on the activated surfaces, as observed in Fig. 2. In either case, the atomic diffusion at the interface, presumably assisted by the point defects introduced in the surface activation process, would be a key

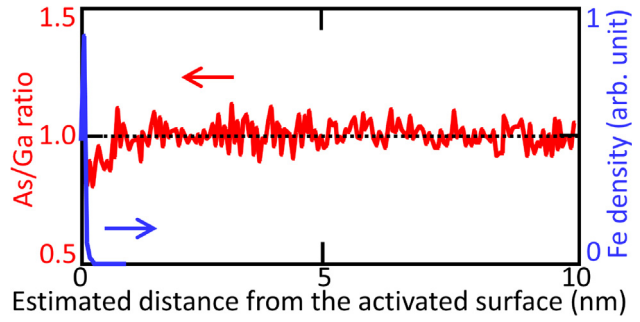

Fig. 3. Depth profile of the As/Ga ratio and Fe density in GaAs annealed at 400 °C after the surface activation process, obtained by TOF-SIMS.

concept of SAB, by which we can fabricate tough heterointerfaces at low temperature. The key concept of SAB is finally the activation itself which is not only needed to remove the surface oxides and to create the dangling bonds but also to enhance the atomic diffusivity.

The total density depletes at the interface, indicating the introduction of vacancies. Since the density profile for Ga atoms can be explained with a simple diffusion model for a uniform semi-finite source, Ga vacancies beneath the activated GaAs surfaces would be negligible, as observed in SAB-fabricated GaAs/GaAs interfaces (see Fig. S2(b) in the SM). Similarly, the density of Si vacancies beneath the activated Si surfaces can be negligible, although a small amount of Si vacancies would be introduced (see Fig. S3(c) in the SM). Therefore, the density depletion is mainly due to As vacancies beneath the activated GaAs surfaces shown in Fig. 1.

3.2. 400 °C annealed GaAs/Si heterointerfaces

When an activated GaAs surface is annealed at 400 °C, the As/Ga ratio is almost 1.0 at any depths from the surface (Fig. 3), except for the outermost surface [43], by TOF-SIMS. Comparing the TOF-SIMS data of as-bonded and 400 °C annealed surfaces, we hypothesize that As vacancies disappear due to the recombination with As interstitials via their migration at 400 °C. In other words, Frenkel-type defects on the As sites can be annihilated at this temperature. This annihilation would be correlated with the depletion of the density of interface states by 400 °C annealing [24].

Fig. 4(a) shows a HAADF-STEM image of a GaAs/Si heterointerface after 400 °C annealing. Parts of amorphous Si are recrystallized during the annealing, and the thickness of the amorphous layer is decreased. The ratio between the As density and the Ga one, As/Ga, is almost 1.0 in the GaAs side (Fig. 4(b)), due to the annihilation of Frenkel-type defects on the As sites (Fig. 3). Although the atomic intermixing across the interface would proceed in the annealing process, the excess Si atoms in GaAs and the excess Ga and As atoms in Si do not increase so much (Fig. 4(b)). Most excess atoms are confined in a narrow region nearby the interface, and their densities seem to be saturated. This result can be explained with a transient enhancement model that excess atoms can diffuse nearby the interface at which point defects are introduced, while they are immobile in a lack of the defects by annealing. Similarly, in the annealing process, Fe atoms do not exhibit apparent diffusion around the heterointerface (Fig. 4(b)) [44], as well as around GaAs/GaAs (see Fig. S2(d) in the SM) and Si/Si (see Fig. S3(e) in the SM) interfaces. It is also speculated that, the residual Ar atoms, locating at the interstitial sites as Fe impurities, could be stable during the low temperature annealing. The mechanical strength of the interface, correlated with the thickness of the gradient layer, would be optimized by controlling the SAB condition.

The total density across the interface shows that most vacancies are annihilated by 400 °C annealing (grey curve in Fig. 4(b)). They would locate on the As site in GaAs, since the As/Ga ratio is recovered to 1.0 by the annealing as observed in Figs. 3 and 4(b), as well as in SAB-fabricated GaAs/GaAs interfaces (see Fig. S2(d) in the SM). Also, small amount of the annihilated vacancies would locate in Si, as observed in SAB-fabricated Si/Si interfaces (see Fig. S3(f) in the SM). This structural change would result in the reduction of the interface resistance [14]. The resistances for SAB-fabricated GaAs/Si (10^{-1} Ωcm^2) [14] and GaAs/GaAs (10^{1} Ωcm^2) [26] interfaces are much higher in comparison with the Si/Si interfaces fabricated with similar SAB conditions (10^{-3} Ωcm^2) [23]. Also, impurity atoms such as Fe and Ar atoms can degrade the electronic properties via the introduction of defect levels. They would not, however, correlate with the recovery of the electronic properties by 400 °C annealing, since their density and distribution seem to be unchanged during the annealing process. Therefore, the resistance of SAB-fabricated GaAs/Si interfaces would be originated mainly from the As defects.

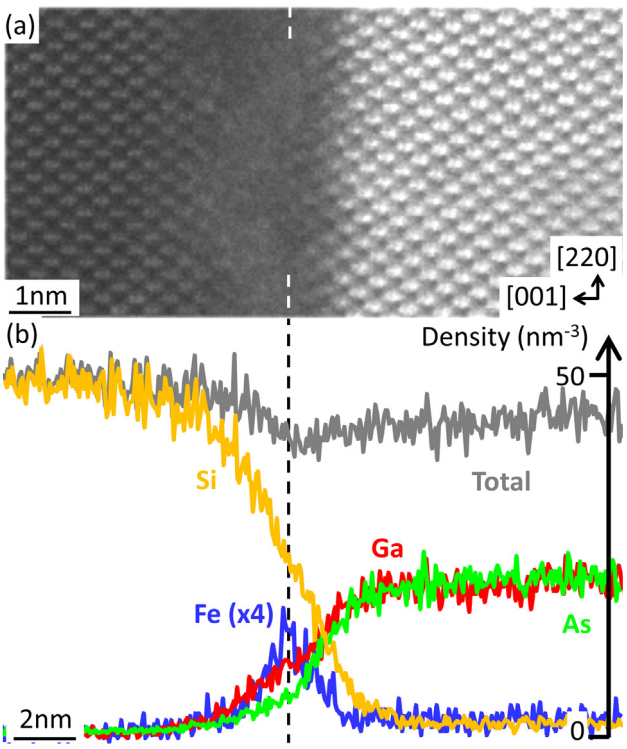

Fig. 4. (a) HAADF-STEM of a 400 °C-annealed GaAs/Si interface. (b) Density profiles across the interface for As (the green curve), Ga (red), Si (orange), Fe (blue), and all kinds of atoms (grey), obtained by EDX. (For interpretation of the references to colour in this figure legend, the reader is referred to the web version of this article.)

4. Conclusion

Atomic intermixing at the SAB-fabricated GaAs/Si heterointerfaces, presumably via the transient enhanced diffusion assisted by the point defects introduced in the surface activation process, is confirmed in the bonding process at RT. The defect-assisted atomic diffusion, as well as the formation of atomically clean and activated surfaces, would be the key concept of SAB, by which we can fabricate tough heterointerfaces of dissimilar materials at RT. On the other hand, those defects, especially Frenkel-defects on the As sites, can degrade the interface resistance. Therefore, we need to optimize the trade-off relationship between the chemical bonding strength and the interface resistance, determined by the activated surfaces before bonding, by controlling SAB conditions.

CRediT authorship contribution statement

Yutaka Ohno: Conceptualization, Methodology, Formal analysis,

Resources, Writing - original draft, Writing - review & editing. **Jianbo Liang:** Investigation, Validation. **Naoteru Shigekawa:** Resources, Writing - review & editing. **Hideto Yoshida:** Investigation, Validation. **Seiji Takeda:** Resources. **Reina Miyagawa:** Investigation, Validation, Formal analysis. **Yasuo Shimizu:** Investigation, Validation, Formal analysis. **Yasuyoshi Nagai:** Resources, Writing - review & editing.

Declaration of Interest Statement

The authors declare that they have no known competing financial interests or personal relationships that could have appeared to influence the work reported in this paper.

Acknowledgments

A part of this work is supported by JST/CREST, Japan, Grant No. JPMJCR17J1 (2017-2023), and JSPS/KAKENHI, Japan, Grant No. 18K05009 (2018-2021). Specimen preparations by LT-FIB and CMP are, respectively, supported at the Oarai Center and at the Laboratory of Alpha-Ray Emitters, under the GIMRT Program in IMR, Tohoku University, Japan (Proposal Nos. 19M0037 and 19M0404). X-STEM is performed at "Network Joint Research Center for Materials and Devices: Dynamic Alliance for Open Innovation Bridging Human, Environment and Materials" in ISIR, Osaka University, Japan (Proposal No. 20191240). SRIM calculations are assisted by Dr. Sosuke Kondo in IMR, Tohoku University, Japan.

Appendix A. Supplementary material

Supplementary data to this article can be found online at https://doi.org/10.1016/j.apsusc.2020.146610.

References

[1] T. Suga, Y. Takahashi, H. Takagi, B. Gibbesch, G. Elssner, Structure of Al/Al and Al/Si_3N_4 interfaces bonded at room temperature by means of the surface activation method, Acta Metall. Mater. 40 (1992) S133–S137.
[2] B. Imbert, P. Gondcharton, L. Benaissa, D. Mariolle, G. Rodriguez, C. Guedj, D. Radisson, F. Fournel, H. Moriceau, Initial stages of interface closure for metal and metal-oxide bonding, in: Book of Abstracts of the Waferbond'15 conference, 2015, pp.127–128: https://inplas.de/files/5793_Book_of_Abstract_WaferBond15_gkac48.pdf.
[3] J. Liang, S. Masuya, M. Kasu, N. Shigekawa, Realization of direct bonding of single crystal diamond and Si substrates, Appl. Phys. Lett. 110 (2017) 111603.
[4] E. Higurashi, K. Okumura, K. Nakasuji, T. Suga, Surface activated bonding of GaAs and SiC wafers at room temperature for improved heat dissipation in high-power semiconductor lasers, Jpn. J. Appl. Phys. 54 (2015) 030207.
[5] T. Suga, F. Mu, M. Fujino, Y. Takahashi, H. Nakazawa, K. Iguchi, Silicon carbide wafer bonding by modified surface activated bonding method, Jpn. J. Appl. Phys. 54 (2015) 030214.
[6] J. Liang, S. Nishida, M. Arai, N. Shigekawa, Effects of thermal annealing process on the electrical properties of p^+-Si/n-SiC heterojunctions, Appl. Phys. Lett. 104 (2014) 161604.
[7] J. Liang, S. Shimizu, M. Arai, N. Shigekawa, Determination of band structure at GaAs/4H-SiC heterojunctions, ECS Trans. 75 (2016) 221–227.
[8] N. Shigekawa, J. Liang, N. Watanabe, A. Yamamoto, Fabrication of nitride/Si tandem cell structures with low environmental burden by surface activated bonding, Phys. Status Solidi C 11 (2014) 644–647.
[9] F. Mu, Y. Morino, K. Jerchel, M. Fujino, T. Suga, GaN-Si direct wafer bonding at room temperature for thin GaN device transfer after epitaxial lift off, Appl. Surf. Sci. 416 (2017) 1007–1012.
[10] R. Takigawa, E. Higurahi, T. Asano, Surface activated bonding of $LiNbO_3$ and GaN at room temperature, ECS Trans. 86 (2018) 207–216.
[11] H. Takagi, R. Maeda, N. Hosoda, T. Suga, Transmission electron microscope observations of Si/Si interface bonded at room temperature by Ar beam surface activation, Jpn. J. Appl. Phys. 38 (1999) 1589–1594.
[12] G. Kono, M. Fujino, D. Yamashita, K. Watanabe, M. Sugiyama, Y. Nakano, T. Suga, Effect of ion species for the surface activated bonding of GaAs wafers on the characteristics of the bonded interfaces, Proc. IECP-IAAC (2015) 478–481.
[13] M. Morimoto, J. Liang, S. Nishida, N. Shigekawa, Effects of annealing on electrical properties of Si/Si junctions by surface-activated bonding, Jpn. J. Appl. Phys. 54 (2015) 030212.
[14] J. Liang, L. Chai, S. Nishida, M. Morimoto, N. Shigekawa, Investigation on the interface resistance of Si/GaAs heterojunctions fabricated by surface-activated bonding, Jpn. J. Appl. Phys. 54 (2015) 030211.
[15] K. Derendorf, S. Essig, E. Oliva, V. Klinger, T. Roesener, S.P. Philipps, J. Benick, M. Hermle, M. Schachtner, G. Siefer, W. Jager, F. Dimroth, Fabrication of GaInP/GaAs//Si solar cells by surface activated direct wafer bonding, IEEE J. Photovolt. 3 (2013) 1423–1428.
[16] N. Shigekawa, J. Liang, R. Onitsuka, T. Agui, H. Juso, T. Takamoto, Current–voltage and spectral-response characteristics of surface-activated-bonding-based InGaP/GaAs/Si hybrid triple-junction cells, Jpn. J. Appl. Phys. 54 (2015) 08KE03.
[17] H. Liu, Z. Ren, Z. Liu, A.G. Aberle, T. Buonassisi, I.M. Peters, The realistic energy yield potential of GaAs-on-Si tandem solar cells: a theoretical case study, Opt. Express 23 (2015) A382–A390.
[18] M. Yamaguchi, K.-H. Lee, K. Araki, N. Kojima, Y. Ohshita, Potential and activities of III-V/Si tandem solar cells, ECS J. Sol. State Sci. Technol. 5 (2016) Q68–Q73.
[19] Z. Ren, H. Liu, Z. Liu, C.S. Tan, A.G. Aberle, T. Buonassisi, I.M. Peters, The GaAs/GaAs/Si solar cell – towards current matching in an integrated two terminal tandem, Sol. Energy Mater. Sol. Cells 160 (2017) 94–100.
[20] J.C.C. Fan, B.Y. Tsaur, B.J. Palm, Optimal design of high-efficiency tandem cells, In: Conf. Record 16th IEEE Photovoltaic Specialists Conf. (IEEE, New York), 1982, pp. 692.
[21] J. Liang, S. Nishida, M. Morimoto, N. Shigekawa, Surface-activating-bonding-based low-resistance Si/III-V junctions, Electron. Lett. 49 (2013) 830–832.
[22] K. Nishioka, T. Takamoto, T. Agui, M. Kaneiwa, Y. Uraoka, T. Fuyuki, Evaluation of InGaP/InGaAs/Ge triple-junction solar cell and optimization of solar cell's structure focusing on series resistance for high-efficiency concentrator photovoltaic systems, Sol. Energy Mater. Sol. Cells 90 (2006) 1308–1321.
[23] S. Essig, F. Dimroth, Fast atom beam activated wafer bonds between n-Si and n-GaAs with low resistance, ECS J. Solid State Sci. Technol. 2 (2013) Q178–Q181.
[24] L. Chai, J. Liang, N. Shigekawa, Effects of annealing on the electrical characteristics of GaAs/GaAs junctions by surface-activated bonding, Jpn. J. Appl. Phys. 55 (2016) 068002.
[25] Y. Kurashima, A. Maeda, H. Takagi, Characterization of bonding interface prepared by room-temperature Si wafer direct bonding using the surface smoothing effect of a Ne fast atom beam, Microelectron. Eng. 118 (2014) 1–5.
[26] H. Takagi, R. Maeda, T.R. Chung, N. Hosoda, T. Suga, Effect of surface roughness on room-temperature wafer bonding by Ar beam surface activation, Jpn. J. Appl. Phys. 37 (1998) 4197–4203.
[27] Y. Ohno, H. Yoshida, S. Takeda, J. Liang, N. Shigekawa, Intrinsic microstructure of Si/GaAs heterointerfaces fabricated by surface-activated bonding at room temperature, Jpn. J. Appl. Phys. 57 (2018) 02BA01.
[28] Y. Ohno, H. Yoshida, N. Kamiuchi, R. Aso, S. Takeda, Y. Shimizu, Y. Nagai, J. Liang, N. Shigekawa, Impact of focused ion beam on structural and compositional analysis of interfaces fabricated by surface activated bonding, Jpn. J. Appl. Phys. 59 (2020) SBBB05.
[29] Y. Shimizu, N. Ebisawa, Y. Ohno, J. Liang, N. Shigekawa, K. Inoue, Y. Nagai, Atom probe tomography of GaAs homointerfaces fabricated by surface-activated bonding, Proc. 6th Int. IEEE Workshop on Low Temperature Bonding for 3D Integration, 2019, p. 56.
[30] Y. Ohno, In-situ analysis of optoelectronic properties of twin boundaries in AlGaAs by polarized cathodoluminescence spectroscopy in a TEM, J. Electron Microsc. 59 (2010) S141–S147.
[31] Y. Ohno, K. Inoue, K. Kutsukake, M. Deura, T. Ohsawa, I. Yonenaga, H. Yoshida, S. Takeda, R. Taniguchi, H. Otsubo, S.R. Nishitani, N. Ebisawa, Y. Shimizu, H. Takamizawa, K. Inoue, Y. Nagai, Nanoscopic mechanism of Cu precipitation at small-angle tilt boundaries in Si, Phys. Rev. B 91 (2015) 235315.
[32] Y. Ohno, K. Inoue, Y. Tokumoto, K. Kutsukake, I. Yonenaga, N. Ebisawa, H. Takamizawa, Y. Shimizu, K. Inoue, Y. Nagai, H. Yoshida, S. Takeda, Three-dimensional evaluation of gettering ability of Σ3{111} grain boundaries in silicon by atom probe tomography combined with transmission electron microscopy, Appl. Phys. Lett. 103 (2013) 102102.
[33] The Stopping and Range of Ions in Matter (SRIM) www.srim.org.
[34] P. Rajput, A. Gupta, S. Rajagopalan, A.K. Tyagi, Fe diffusion in amorphous Si studied using x-ray standing wave technique, AIP Adv. 2 (2012) 012159.
[35] J. Crank, The Mathematics of Diffusion, Clarendon Press, Oxford, 1975.
[36] T. Ahlgren, J. Likonen, J. Slotte, J. Raisanen, M. Rajatora, J. Keinonen, Concentration dependent and independent Si diffusion in ion-implanted GaAs, Phys. Rev. B 56 (1997) 4597–4603.
[37] I.A. Prudaev, S.S. Khludkov, Diffusion and solubility of electrically active iron atoms in gallium arsenide, Russian Phys. J. 51 (2008) 1157–1160.
[38] Y.M. Haddara, J.C. Bravman, Transient diffusion of beryllium and silicon in gallium arsenide, Annu. Rev. Mater. Sci. 28 (1998) 185–214.
[39] S. Haridoss, F. Beniere, M. Gauneau, A. Rupert, Diffusion of gallium in silicon, J. Appl. Phys. 51 (1980) 5833–5837.
[40] R.B. Fair, J.C.C. Tsai, The diffusion of ion-implanted arsenic in silicon, J. Electrochem. Soc. 122 (1975) 1689–1695.
[41] M. Uematsu, K. Wada, Recombination-enhanced impurity diffusion in Be-doped GaAs, Appl. Phys. Lett. 58 (1991) 2015–2017.
[42] A.M. Fecioru, S. Senz, U.M. Gosele, Room temperature UHV bonding of Si to GaAs, in: Proc. Int. Symp. Semiconductor Wafer Bonding VIII: Science, Technology, Appl., Electrochem. Soc., 2005, pp. 385–391.
[43] Unlike at GaAs/GaAs homointerfaces locating inside the bonded wafers, the As/Ga ratio at the bare GaAs surface annealed at 400°C becomes below 1.0 since small amount of As atoms would evaporate during the annealing.
[44] As observed in Fig. 3, when an activated GaAs wafer is annealed without bonding, Fe atoms would segregate on the surface, presumably due to a low solubility.